



## ELECTRIC FIELD DISTRIBUTION IN SPARK PLUGS INSULATORS – MODELING AND COMPUTER SIMULATION

Bernard FRYŠKOWSKI

Faculty of Electrical Engineering, Warsaw University of Technology

Plac Politechniki 1, Warsaw, Poland, +48 22 621 98 25, [bernard.fryskowski@ee.pw.edu.pl](mailto:bernard.fryskowski@ee.pw.edu.pl)

### Abstract

Automotive spark plugs are essential ignition circuit components being of importance for combustion engine reliability and performance. The majority of spark plugs have ribbed ceramic insulator to ensure high resistance along the surface from the terminal to the metal shell to minimize leakage current and to provide flashover protection. The leakage current intensity depends on electric field distribution, physical insulator properties and such factors as humidity, insulator contamination or defects in insulation material. Furthermore, leakage current not infrequently interferes with discharge process causing misfire effect being harmful to exhaust manifold components, mainly to catalytic converters. This paper presents simulation results of electric field distribution in ceramic insulator, in silicone rubber boot and in space surrounding a spark plug. Assuming that a spark plug can be considered as an object having cylindrical symmetry the electric field distribution was calculated for a two-dimensional case in accordance with Laplace's and Poisson's equations. In this paper, the finite difference method (FDM) for the solution of the Laplace's equation was applied. The FDM algorithm based on the Liebmann's method was developed in the MATLAB environment. Presented simulation results can be helpful to automotive spark plugs and high-tension cables manufacturers interested in improvement of insulating properties.

Keywords: spark plugs, automotive ignition systems, ceramic insulators, electric field, finite difference method

## ROZKŁAD POLA ELEKTRYCZNEGO W IZOLATORACH ŚWIEC ZAPŁONOWYCH – MODELOWANIE I SYMULACJA KOMPUTEROWA

### Streszczenie

Samochodowe świece zapłonowe zaliczane są do podzespołów układów zapłonowych ważnych z punktu widzenia niezawodności i sprawności silnika spalinowego. Większość świec zapłonowych posiada izolator ceramiczny z barierami zapewniający wysoką wartość rezystancji między zaciskiem elektrody środkowej i korpusem w celu ograniczenia natężenia prądu upływu i zapobiegania zjawisku wyładowania powierzchniowego. Natężenie prądu upływu uzależnione jest od rozkładu pola elektrycznego, właściwości fizycznych izolatora i takich czynników jak wilgotność, zanieczyszczenie lub uszkodzenia materiału izolacyjnego. Nierzadko prąd upływu zakłóca przebieg procesu wyładowania iskrowego prowadząc do wypadania zapłonów, które stanowi zagrożenie dla elementów układu wydechowego, głównie dla katalizatorów. W treści artykułu przedstawiono wyniki symulacji komputerowej rozkładu pola elektrycznego w izolatorze, silikonowej osłonie izolacyjnej oraz w przestrzeni otaczającej świecę zapłonową. Przyjmując założenie, że świecę zapłonową charakteryzuje symetria osiowa, wyznaczono rozkład pola elektrycznego w postaci dwuwymiarowej korzystając z oprogramowania MATLAB. Obliczenia wykonano rozwiązując równania Laplace'a i Poissona metodą różnic skończonych przy zastosowaniu procedury Liebmann. Przedstawione wyniki symulacji komputerowej mogą być przydatne dla producentów samochodowych świec i przewodów zapłonowych zainteresowanych poprawą właściwości izolacyjnych.

Słowa kluczowe: świece zapłonowe, układy zapłonowe, izolatory ceramiczne, pole elektryczne, metoda różnic skończonych

## 1. INTRODUCTION

Spark plugs are dominant automotive parts responsible for lower exhaust emissions and fuel consumption. Although spark plugs are an important component of automotive ignition system operating in high-voltage and high-pressure circumstances, only a few of significant changes in their construction were observed in recent years. The changes were related in most cases to electrodes number, location, geometry and materials the electrodes are made of [1, 2, 3].

Many studies have been focused so far on spark plug temperature, electric parameters, cylinder pressure or electromagnetic field modeling inside the combustion chamber, especially in the air gap [4-13]. Nevertheless, the spark discharge energy may be affected by some effects observed outside the combustion chamber e.g. ceramic insulator flashover or leakage current flow. In this paper electric field surrounding a ribbed spark plug insulator was analyzed by means of computer simulation. The objectives were to perform scalar potential and electric field strength computer simulations inside

and in the vicinity of ceramic insulator and silicone rubber boot.

The main function of automotive spark plugs insulators is to protect the high-voltage part of the ignition circuit from leakage current, surface flash-over effect and parasitic discharges resulting in lower spark energy or misfire effect. The insulators are made of ceramic containing sintered alumina (90-95%), magnesium oxide, sodium oxide and silicon dioxide [14, 15]. The ceramic material is applied to provide for sufficient mechanical strength and durability because of high pressure inside the combustion chamber.

The distribution of the local electric field is of practical importance considering a possibility of partial discharge effect between center and ground electrodes across the ceramic or on the outside of the insulator. On the other hand the electric field distribution is an important factor with regard to ceramic insulator contamination problems and silicone rubber boots degradation.

## 2. ELECTRIC FIELD MODELING – MATHEMATICAL BACKGROUND

The physical aspect of spark plug insulator's electric field modeling is usually employed in obtaining appropriate differential equations, domain (solution regions), boundary conditions, numerical procedures and in evaluation of numerical solution accuracy. For electric potential and electric field strength modeling purpose, it is convenient to apply a two-dimensional second-order partial differential equation solved using methods based on analytical or numerical techniques like finite difference or finite element algorithms. In this paper spark plug insulator's electric field distribution was modeled as an interior problem. Hence, several bounded solution regions were specified as shown in figure 1.

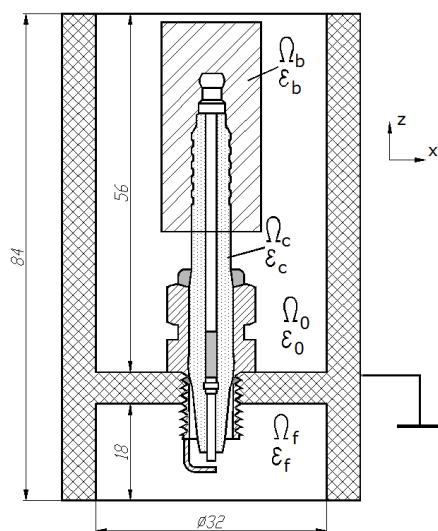


Fig. 1 Spark plug electric field solution regions

The specified solution regions are:  $\Omega_0$  – a space surrounding upper part of the spark plug, outside the

combustion chamber, with air dielectric constant  $\epsilon_0$ ,  $\Omega_b$  – insulating cover (spark plug boot) made of silicone rubber having relative permittivity  $\epsilon_b$ ,  $\Omega_c$  – ceramic insulator (alumina relative permittivity  $\epsilon_c$ ),  $\Omega_f$  – combustion chamber internal space with air-fuel mixture dielectric constant  $\epsilon_f$ .

The electric field of spark plug insulators can be considered at the moment prior to discharge effect as a quasi-electrostatic field. Assuming that the electric potential is steady and no leakage current flow is observed the Laplace's equation governing electric potential  $V$  of a ceramic insulator surrounding the center electrode of a spark plug is given as:

$$\nabla^2 V = 0 \quad (1)$$

In materials with specified electric charge distribution electric potential is determined by Poisson's equation:

$$\nabla^2 V = -\frac{\rho_v}{\epsilon} \quad (2)$$

where  $\rho_v$  and  $\epsilon$  are electric volume charge density and dielectric permittivity respectively.

The surface charge of the center electrode imposes the Neumann boundary condition:

$$\frac{\partial V}{\partial n} = 0 \quad (3)$$

where  $\frac{\partial V}{\partial n}$  is the directional derivative of  $V$  along the outward normal to the boundary. The Dirichlet boundary condition  $V = 0$  applied to the equations (1) and (2) was sufficient for the metal shell and conductive engine parts surrounding the spark plug. Laplace's equation solution can be found by means of a finite difference approximation constructed according to the formula [16]:

$$V(i, j) = \frac{1}{4} \left[ V(i, j-1) + V(i, j+1) + \left( \frac{2i-1}{2i} \right) V(i-1, j) + \left( \frac{2i+1}{2i} \right) V(i+1, j) \right] \quad (4)$$

where  $i$  and  $j$  are grid points indexes. Furthermore, the electric field strength can be calculated as the gradient of the scalar electric potential  $V$ :

$$E = -\nabla V \quad (5)$$

The solutions to the equations (1), (2) and (5) governing electric potential and electric field strength distributions were found using MATLAB computer program based on finite difference algorithm (FDM) and Liebmann's method [17]. The program was applied to simulate the electric field distribution for two cases – insulators in the absence of charge (Laplace's equation) and non-ideal dielectric (Poisson's equation).

**3. SIMULATION MODEL VERIFICATION AND VALIDATION**

The accuracy level of calculations performed by FDM algorithm application is essential when determining the acceptability of the approximation results. The accuracy has been verified by simulation results comparison with known exact analytical solutions. For this purpose the scalar potential and electric field strength distribution inside a three-layer ideal cylindrical capacitor shown in figure 2 were calculated analytically and simulated using the FDM method.

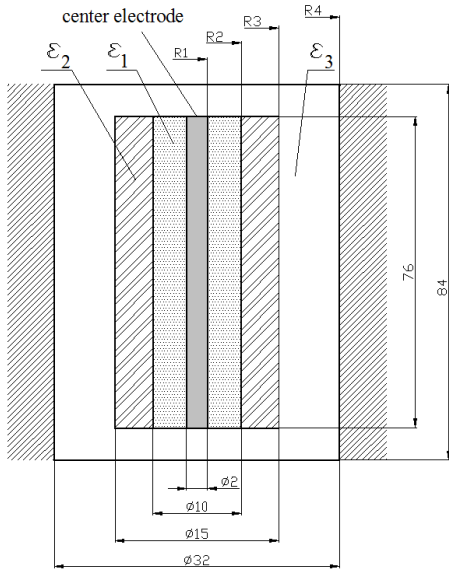


Fig. 2 Three-layer ideal cylindrical capacitor model applied to verify the FDM algorithm

The first dielectric layer is ceramic insulator, the next one – silicone rubber, the third layer is air so that  $\epsilon_1 = \epsilon_c$ ,  $\epsilon_2 = \epsilon_b$ ,  $\epsilon_3 = \epsilon_0$ . Exact scalar potential and electric field strength formulas were derived from a steady state logarithmic solution to Laplace’s equation for a multi-layer cylindrical capacitor, namely

$$V_i(r) = c_{i1} \ln r + c_{i2} \tag{6}$$

$$E_i(r) = \frac{-U}{\epsilon_i M r} \tag{7}$$

where  $U$  is the voltage across the center and external capacitor electrodes,  $c_{i1}$  and  $c_{i2}$  are the constants for  $i$ -th layer. The  $M$  coefficient considering relative permittivity of dielectric layers and capacitor geometry is given by:

$$M = \sum_{i=1}^3 \frac{1}{\epsilon_i \ln \frac{R_{i+1}}{R_i}} \tag{8}$$

Imposing the Neumann and Dirichlet boundary conditions the potential and electric field strength equations for all dielectric layers become:

$$V_1(r) = \frac{U}{M} \left( \frac{1}{\epsilon_3} \ln \frac{R_3}{R_2} + \frac{1}{\epsilon_2} \ln \frac{R_2}{R_1} + \frac{1}{\epsilon_1} \ln \frac{R_1}{r} \right) \tag{9}$$

$$E_1(r) = \frac{-U}{\epsilon_1 M r} \tag{10}$$

$$V_2(r) = \frac{U}{M} \left( \frac{1}{\epsilon_3} \ln \frac{R_3}{R_2} + \frac{1}{\epsilon_2} \ln \frac{R_2}{r} \right) \tag{11}$$

$$E_2(r) = \frac{-U}{\epsilon_2 M r} \tag{12}$$

$$V_3(r) = \frac{U}{M \epsilon_3} \ln \frac{R_3}{r} \tag{13}$$

$$E_3(r) = \frac{-U}{\epsilon_3 M r} \tag{14}$$

One of the most important factors affecting the convergence and accuracy of the FDM approximation is the number of iterations. The number of iteration  $k$  is acceptable if the maximal error at grid point  $(i, j)$  does not exceed  $\epsilon$ . Hence, the approximation process is stopped after  $k+1$  iterations if [18]:

$$\max |V^{k+1}(i, j) - V^k(i, j)| \leq \epsilon \tag{15}$$

Assuming that the maximal error required at grid point  $(i, j)$  should not exceed 0.01 V the number of needed iterations was 17356. The maximal error after 25000 iterations was equal 0.0012 V. Numerical calculation results compared with analytic solutions are shown in figure 3 in order to test the accuracy of the FDM algorithm applied to the simulation of electric field distribution.

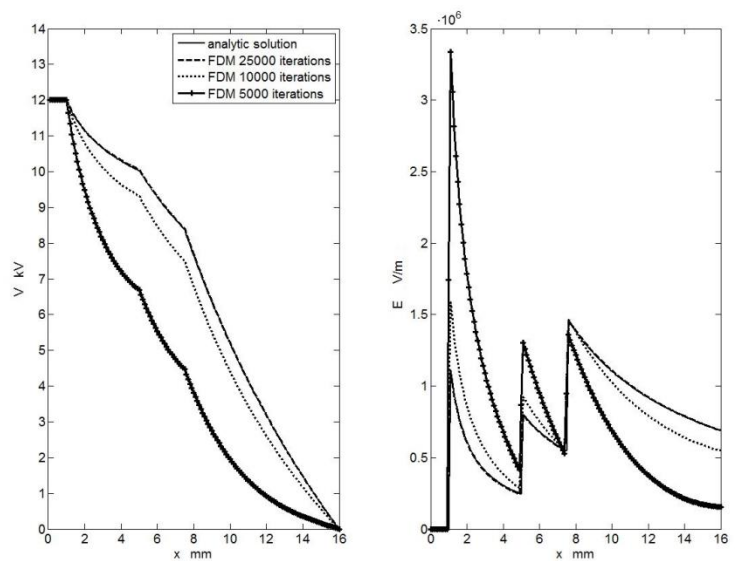


Fig. 3 Scalar potential and electric field strength numeric calculations compared with analytic solution

The relative percentage difference was evaluated to compare in a quantitative way the analytic solution with the simulation results obtained using the proposed FDM algorithm. The percentage error  $\delta$  can be derived from:

$$\delta = \left| \frac{V_A - V_{FDM}}{V_A} \right| \cdot 100\% \quad (16)$$

where  $V_A$  and  $V_{FDM}$  are scalar potentials calculated according to analytic method and FDM respectively. The appropriate results of error calculation for 5000, 10000 and 25000 iterations are shown in table 1.

Table 1 Simulation results versus analytic solution; maximal percentage error

number of iterations	5000	10000	25000
scalar potential	64.79%	20.87%	0.39%
electric field strength	152.53%	42.72%	2.03%

The scalar potential and electric field strength distributions were well represented for 25000 iterations with the relative error smaller than 0.5% and 2.5% respectively. Greater differences were observed for relatively low number of iterations i.e. less than 10000. Therefore, all numeric simulations results presented in this paper were achieved at 25000 iterations. Other sources of FDM uncertainty are roundoff errors and truncation errors. The roundoff errors depend on arithmetic precision of used computer. The way to reduce the truncation errors is to employ finer mesh size resulting in smaller approximation spatial step size. However, refined mesh causes larger number of arithmetic operations increasing the roundoff error [16].

#### 4. SPARK PLUG INSULATOR'S ELECTRIC FIELD DISTRIBUTION – SIMULATION RESULTS

The discussed FDM algorithm has been applied to the Bosch FR7DC spark plug shown in figure 4.

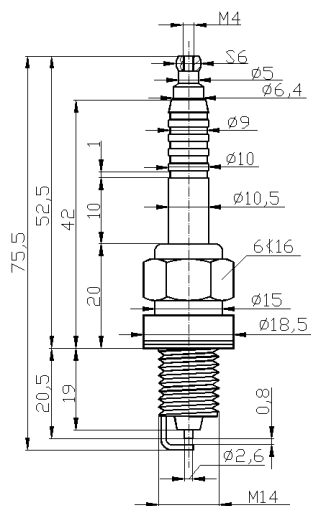


Fig. 4 Spark plug Bosch FR7DC

The boundary conditions were defined taking into consideration that the conductive parts of combustion engine are connected to the negative pole of the battery. Therefore, the electric potential of the cylinder head equals 0V. The Bosch FR7DC spark plug was installed in the cylinder head in accordance with dimensioning shown in figure 1. A cylindrical connector was applied to connect the terminal nut to a high-tension cable. The FDM approximation spatial step size (square mesh size) was 0.1 mm. The computer simulation of electric field distribution was provided according to input physical parameters [19, 20] given in table 2.

Table 2 Relative permittivity values applied for simulation of electric field distribution

Relative permittivity	Value
alumina	9
silicone rubber	2.7
gasoline	2

The nominal air gap width of the FR7DC spark plug was 0.8 mm. Hence, the high voltage supplied to the center electrode was 12 kV as the minimum voltage required for breakdown at the air-gasoline mixture dielectric strength of  $15 \cdot 10^6$  V/m [21]. The spark plug boot was represented by a cylinder having internal diameter 10.5 mm, external diameter 15 mm, length 32 mm. Scalar potential and electric field strength simulation results for the spark plug FR7DC are shown in figure 5.

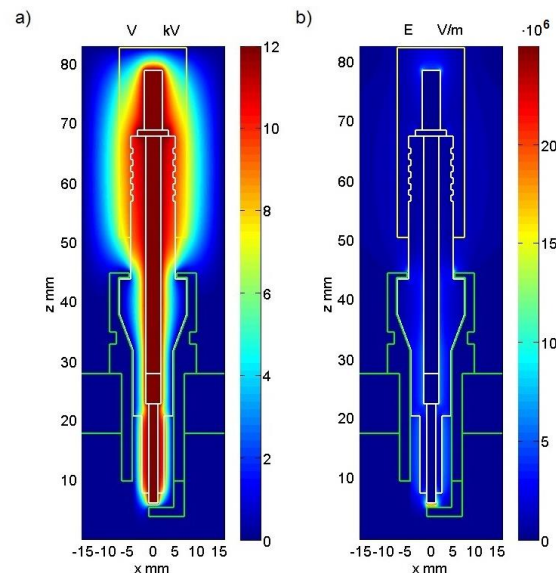


Fig. 5 Scalar potential (a) and electric field strength distribution (b) of the Bosch FR7DC spark plug

The upper part of spark plug insulator along the silicon rubber boot forms a triple layer cylindrical capacitor. Initially, the silicone rubber spark plug boot has been modeled as an ideal insulator (Laplace's equation). It is noticed that the electric potential distribution in the silicon rubber boot along the ceramic insulator is not uniform. As expected,

high electric field strength is observed in the air gap between center and ground electrodes. Especially strong electric field (about  $25 \cdot 10^6$  V/m) occurs at sharp edges of the center electrode – air interface. Some quantitative conclusions can be drawn due to detailed scalar potential and electric field strength analysis in several regions specified in figure 6.

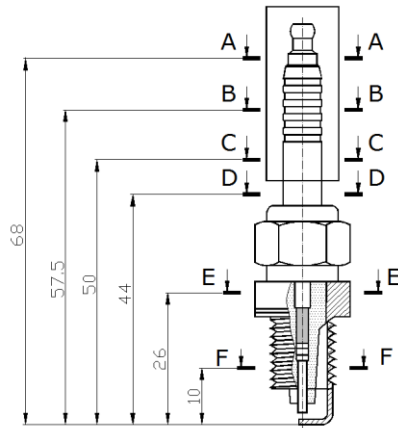


Fig. 6 Regions specified as the basis for quantitative electric field analysis

Regions A-A, D-D and F-F represent double-layer cylindrical capacitors with silicone rubber – air (A-A) and alumina – air interface respectively. Region B-B is a capacitor containing four layers – alumina, air in a rib, silicone rubber and air surrounding the spark plug. Region C-C is equivalent to a cylindrical capacitor having three layers – alumina, silicone rubber and air. Region E-E is a single layer cylindrical capacitor having alumina dielectric only.

High leakage current is often caused by wet or defective silicone rubber boot losing its insulating properties. Consider two following cases:

- ideal insulating properties of ceramic and silicone rubber insulators (Laplace's equation)
- presence of the charge density  $0.003 \text{ C/m}^3$  in silicone rubber boot (Poisson's equation)

Scalar potential and electric field strength distribution simulation results for the FR7DC spark plug in all regions shown in figure 6 calculated with respect to Laplace's and Poisson's equations are presented in figures 7 and 8.

Some differences in potential and electric field strength distribution were noticed in A-A, B-B and C-C regions where the silicone rubber boot is present. The electric potential of silicone rubber insulator has increased by maximal 1.28 kV in case of the charge density presence. Maximal electric field strength increase  $0.28 \cdot 10^6$  V/m was observed in air surrounding the boot. Stronger electric field is able to attract charged oil particles which contaminate insulator's surface. The conductive particles deposited on the ceramic insulator or on the silicone rubber boot may raise the surface conductivity resulting in leakage current or electric arc shunting spark plug electrodes.

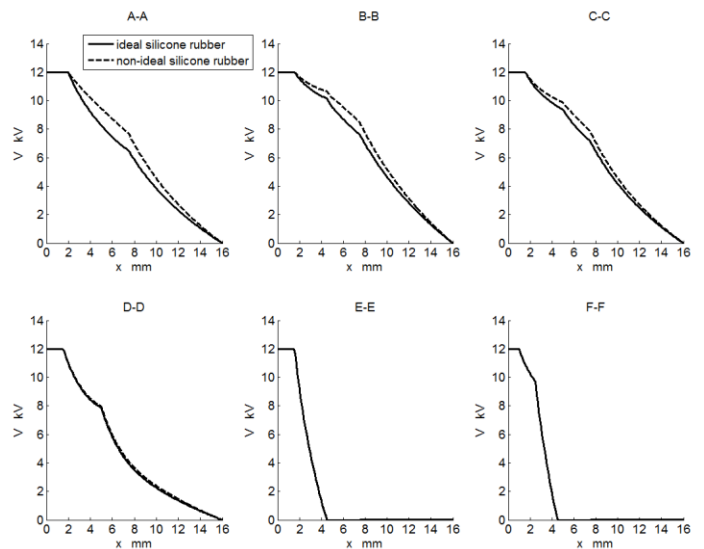


Fig. 7 Bosch FR7DC, potential distribution

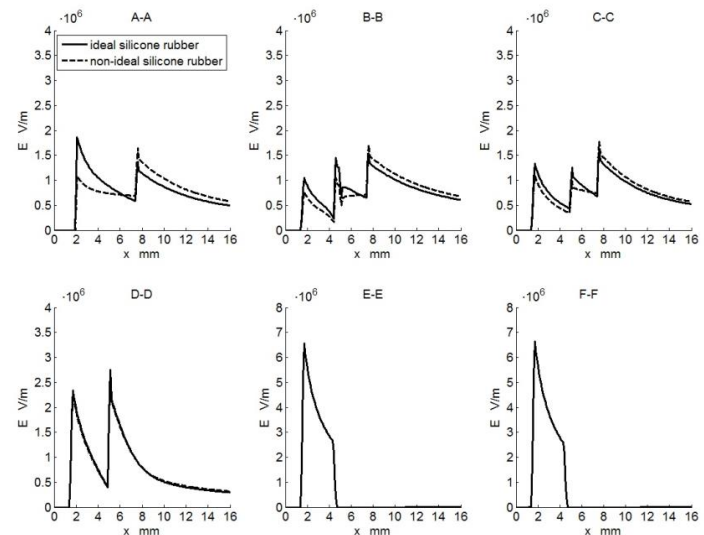


Fig. 8 Bosch FR7DC, electric field strength distribution

According to the simulation results shown in figures 7 and 8 the charge density presence has no significant influence on electric field in the areas D-D, E-E and F-F being relatively far from the silicone rubber boot.

Any shunt resistance occurring as a consequence of fouling effect or insulator contamination affects spark plug's electric field. Scalar potential versus shunt resistance measurement results 10 mm above the FR7DC spark plug insulator surface in the area D-D are shown in table 3.

Table 3 Shunt resistance influence on scalar potential 10 mm above the FR7DC spark plug insulator surface

resistance kΩ	scalar potential kV
161	3.1
122	2.8
102	2.6
81	2.5
71	2.4
61	1.8

Increasing leakage current causes scalar potential decrease. For the potential value 1.8 kV at 61 k $\Omega$  shunt resistance no spark was observed (misfire effect).

## 5. CONCLUSIONS

The accuracy and simplicity of the FDM model discussed in this paper make it useful for estimating electric field distribution in automotive high-voltage insulators. Thus, the proposed model may be applied to electric field analysis in other parts of an ignition system like insulated high-tension cables or ignition coils covers.

The simulation results provide valuable information on the electric field inside and in the vicinity of ceramic insulator and silicone rubber boot. Many studies show that the spark plug electric field analysis inside the combustion chamber is of importance especially because of air-fuel mixture ignition process and ceramic insulator fouling resulting in misfire effect. On the other hand the misfire may be caused by other effects such as parasitic shunt resistance of contaminated external insulator surface or silicone rubber boot degradation.

Vibrations, high temperature and compact design make that practical electric field measurements in the proximity of spark plugs are very difficult to perform. Hence, the computer simulation is an advantageous method to investigate and analyze electric field properties being of importance for ignition circuits efficiency.

## REFERENCES

1. Abdel-Rehim A. A. Impact of spark plug number of ground electrodes on engine stability. *Ain Shams Engineering Journal*, 2013, vol. 4, issue 2, 307–316.
2. Javan S., Alaviyoun S., Hosseini S. V., Ommi F. Experimental study of fine center electrode spark plug in Bi-fuel engines. *Journal of Mechanical Science and Technology*, 2014, vol. 28, no. 3, 1089–1097
3. Linkenheil K., Ruoss H. O., Grau T., Seidel J., Heinrich W. A Novel Spark-Plug for Improved Ignition in Engines with Gasoline Direct Injection (GDI), *IEEE Transactions on Plasma Science*, 2005, vol. 33, no. 5, 696–1702
4. Chih-Lung S., Jye-Chau S., Tsair-Chun L. A Novel Dual-Electrode Plug to Achieve Intensive Electric Field for High Performance Ignition, *Mathematical Problems in Engineering*, 2013, vol. 2013, Article ID 351594, 1-7, doi:10.1155/2013/351594
5. Wang Q., Zheng Y., Yu J., Jia, J. Circuit model and parasitic parameter extraction of the spark plug in the ignition system, *Turkish Journal of Electrical Engineering & Computer Sciences*, 2012, vol.20, no.5, 805-817
6. Bokhary A. Y., Turki A., Ahmad N., Jefri A. H. Simulation of Eccentricity in Spark Plug and its Effects on Combustion Parameters in Spark Ignition Engine, *International Journal of Engineering Science and Technology*, 2012, vol. 4, issue 11, 4676-4686
7. Song J., Sunwoo M. Flame kernel formation and propagation modelling in spark ignition engines, *Proceedings of the Institution of Mechanical Engineers, Part D: Journal of Automobile Engineering*, 2001, vol. 215, 105-114
8. Hnatiuc B., Astanei D., Pellerin S., Hnatiuc M., Faubert F., Ursache M. Electrical Modeling of a Double Spark at Atmospheric Pressure, *International Conference on Optimization of Electrical and Electronic Equipment (OPTIM)*, IEEE, Bran, 2014, 1005–1010
9. Thiele M., Selle S., Riedel U., Warnatz J., Maas U. Numerical Simulation of Spark Ignition Including Ionization, *Proceedings of the Combustion Institute*, 2000, vol. 28, 1177–1185
10. Stevenson R. C., Palma R., Yang C. S., Park S. K., Mi C. Comprehensive Modelling of Automotive Ignition Systems, *SAE Technical Paper Series*, 2007, 2007-01-1589, 1-24
11. Shi Y., Ge H., Reitz R. D. Computational Optimization of Internal Combustion Engines, *Springer Verlag*, London, 2011
12. Song C. Q., Li J., Qu D. W., Yu K. Simulation Study about Dual Spark Plug Position for the CNG Engine Combustion Process, *Advanced Materials Research*, 2013, vols. 712-715, 1197-1200
13. Andreassi L., Cordiner S., Rocco V. Modelling the early stage of spark ignition engine combustion using the KIVA-3V code incorporating an ignition model, *International Journal of Engine Research*, 2003, vol. 4, no. 3, 179-192
14. Brook J. R. Concise encyclopedia of advanced ceramic materials, *Pergamon Press*, 2012, Oxford
15. Imanaka Y. *Advanced Ceramic Technologies & Products*, The Ceramic Society of Japan, Springer, Tokyo, 2012
16. Sadiku M. *Numerical Techniques in Electromagnetics with MATLAB*, CRC Press, Boca Raton, 2009
17. Ames W. F. *Numerical Methods for Partial Differential Equations*, Academic Press Inc., San Diego, 1992
18. Isaacson E., Keller H. B. *Analysis of numerical methods*, John Wiley & Sons, New York, 1994
19. Ashby M. F., Shercliff H., Cebon D. *Materials: engineering, science, processing and design*, Butterworth-Heinemann, Oxford, 2014
20. Arik E., Altan H., Esenturk O. Dielectric Properties of Ethanol and Gasoline Mixtures by Terahertz Spectroscopy and an Effective Method for Determination of Ethanol Content of Gasoline, *Journal of Physical Chemistry*, 2014, 118 (17), 3081–3089, DOI: 10.1021/jp500760t
21. Ida N. *Engineering Electromagnetics*, Springer International Publishing Switzerland, 2015



**Bernard FRYŚKOWSKI,**  
PhD – lecturer and postdoctoral  
researcher at Faculty of Electrical  
Engineering, Warsaw University  
of Technology. Areas of research  
expertise – automotive electrical  
systems, electronics, car  
diagnostics, combustion engines,  
ignition systems, in-vehicle data

transmission networks.